

Reservoir-Fluid Sampling and Characterization— Key to Efficient Reservoir Management

N.R. Nagarajan, M.M. Honarpour, and K. Sampath, ExxonMobil Upstream Research Company

Abstract

Reservoir-fluid properties play a key role in the design and optimization of injection/production strategies and surface facilities for efficient reservoir management. Inaccurate fluid characterization often leads to high uncertainties in in-place-volume estimates and recovery predictions, and hence affects asset value. Reservoir-fluid pressure/volume/temperature (PVT) characterization begins with acquisition of adequate volumes of representative fluid samples followed by PVT-data measurement with strict quality-assurance/quality-control (QA/QC) protocols and phase-behavior modeling through best-practice methods. In this paper, key steps involved in accurate fluid characterization are discussed for a wide spectrum of fluid types ranging from extraheavy oils to highly volatile near-critical fluids and lean gas condensates undergoing a wide range of production processes from simple depletion to complex tertiary recovery. Selection of appropriate sampling methods and tools, design of tool strings, and customizing procedures are demonstrated through these examples. Routine and special laboratory-fluid-analysis strategies for various fluid types and for different production strategies are highlighted. Fluid-modeling techniques including optimum-component selection, accurate C_{7+} characterization, robust Gibb's energy minimization, and gravity/chemical equilibrium calculations are demonstrated through appropriate field examples.

Introduction

Reservoir-fluid PVT properties are critical for efficient reservoir management throughout the life of the reservoir, from discovery to abandonment (See complementary paper by Honarpour et al. 2006.) Reliable PVT properties of in-situ fluids are essential for the determination of in-place volumes

and recovery-factor calculations and are key input to reservoir simulations for technical evaluation of reservoir-development/-depletion plans. Fluid characterization and distribution within the reservoir help in defining reservoir continuity and communication among various zones. Interpretation of well-test data and the design of surface facilities and processing plants require accurate fluid information and its variation with time. In addition to initial reservoir-fluid samples, periodic sampling is necessary for reservoir surveillance.

Reservoir-fluid characterization consists of several key steps: (1) acquisition of representative samples, (2) identification of reliable service laboratories to perform PVT measurements, (3) implementation of QA/QC procedures to ensure data quality, and (4) development of mathematical models to capture fluid-property changes accurately as functions of pressure, temperature, and composition. The fluid type and production processes dictate the type and the volume of required fluid data. This paper outlines recommended sampling techniques, PVT-data-acquisition strategies, and modeling methods and presents field examples covering a wide range of fluid types from heavy oils to lean gas condensates and production processes such as depletion, pressure maintenance, and miscible recovery.

Sampling—Methods, Tools, and Recommended Practice.

The main objective of a successful sampling campaign is to obtain representative fluid samples for determining PVT properties. In addition to PVT samples, adequate volumes should be collected for plant and process analysis, geochemical analysis for fluid-source identification and reservoir continuity, and crude assay for refinery processes. The critical steps in any successful sampling program are avoiding two-phase flow in the reservoir, minimizing fluid contamination introduced by drilling and completion fluids, and preserving sample integrity. A sampling program should focus on the key issues of selecting an appropriate sampling method and associated tools, customizing the tool string, and developing sound sampling, sample-transfer, and QC procedures. In addition, specific sampling issues should be addressed related to fluid type and condition, saturated vs. undersaturated, and fluids with nonhydrocarbon components or fluids containing solid-forming components such as waxes and asphaltenes.

N.R. Nagarajan, SPE, is an engineering associate at ExxonMobil's Upstream Research Company with 22 years of experience in the oil industry. He holds a PhD degree in physics and has served on program committees and the Forum Series for SPE. Mehdi Matt Honarpour, SPE, is a senior engineering adviser with ExxonMobil Upstream Research Company in Houston. He holds BS, MS, and PhD degrees in petroleum engineering from the U. of Missouri. Honarpour served as the Chairperson of SPEREE Review Committee and as the Chairperson of the SPE Special Series Committee. Krishnaswamy Sampath, SPE, is the Reservoir Division Manager at ExxonMobil's Upstream Research Company in Houston. He has served on program committees for the SPE Annual Technical Conference and Exhibition and as a technical editor for SPE journals.

Copyright 2007 Society of Petroleum Engineers
This paper, SPE 103501, is based on paper 101517 presented at the 2006 Abu Dhabi International Petroleum Exhibition & Conference, Abu Dhabi, 5–8 November. **Distinguished Author Series** articles are general, descriptive representations that summarize the state of the art in an area of technology by describing recent developments for readers who are not specialists in the topics discussed. Written by individuals recognized as experts in the area, these articles provide key references to more definitive work and present specific details only to illustrate the technology. **Purpose:** to inform the general readership of recent advances in various areas of petroleum engineering.

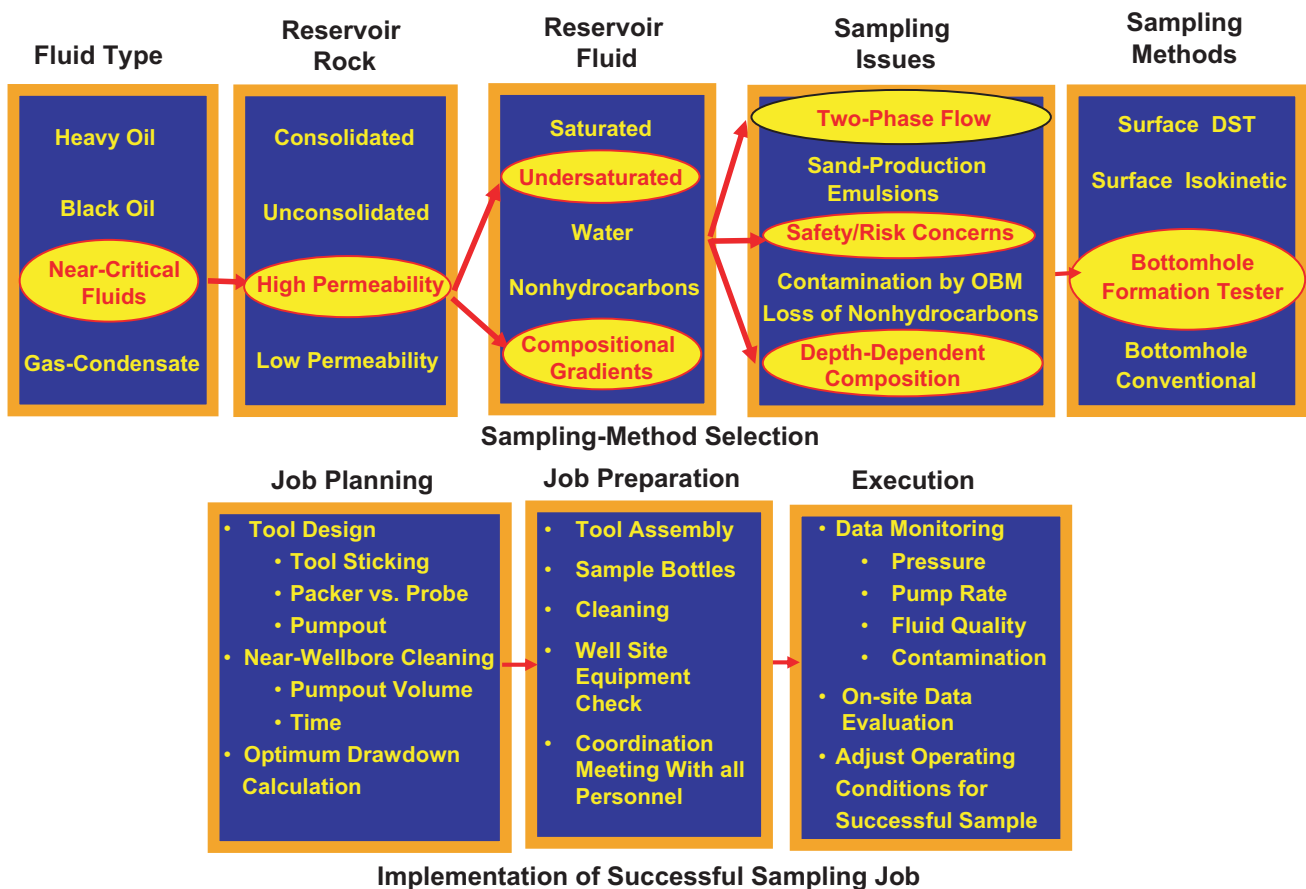


Fig. 1—Reservoir fluid sampling guidelines. OBM=oil-based mud, DST=drillstem test.

Selecting Sampling Method and Tools. The two commonly used sampling methods are bottomhole and surface sampling. Bottomhole sampling attempts to capture samples close to reservoir conditions, while surface sampling aims at capturing gas and oil samples from the separator under stable flow conditions. Separator fluids then are recombined at a measured producing gas/oil ratio (GOR) to prepare representative reservoir fluid. Both methods have challenges and issues that must be overcome to ensure high-quality samples.

In bottomhole-sampling operations, adequate cleaning of near-wellbore regions and controlled drawdown are critical for obtaining uncontaminated representative samples (Witt and Crombie 1999). Controlled drawdown helps avoid two-phase flow in the reservoir. Downhole fluid analyzers are used to monitor sample contamination and ensure single-phase flow prior to sample capture. Accurate calibration of these analyzers is essential for accurate estimate of contamination levels. In surface sampling operation, proper well conditioning with minimum drawdown is the key to acquiring high-quality samples (Witt et al. 1999). Well conditioning requires that the well be flowed at an optimum rate for an extended period of time with a stable producing GOR. Other factors that affect sample quality are separator efficiency and uncertainties in surface oil- and gas-rate measurements.

While bottomhole sampling has the advantage of capturing fluids at reservoir conditions, surface sampling operation has a potential for obtaining cleaner samples as a result of large volumes of fluid production before sampling.

Because a variety of sampling tools and techniques are available, careful thought should be given to tool selection and configuration as well as sampling procedures to tailor them to specific reservoirs and fluids. Fig. 1 provides general sampling guidelines that consist of two parts, sampling-method selection and successful implementation. Selection of a sampling method requires a critical review of reservoir conditions, rock and fluid type, and several relevant sampling issues listed in Fig. 1. Implementation involves details of tool selection and configuration, developing procedures, wellsite execution, and QC. For example, the highlighted items in Fig. 1 are an example of a near-critical-fluid sampling and demonstrate how the rock and fluid conditions and other relevant sampling issues lead to the selection of a bottomhole formation-tester sampling method. Fig. 1 also shows the steps involved in the job planning and preparation. Often, operational considerations, safety issues, and cost are critical in the final decision.

PVT Data—Requirement and QC. The objective of the PVT-data-gathering phase is to obtain reliable high-quality data for

TABLE 1—PVT-DATA REQUIREMENT FOR VARIOUS FLUIDS AND PRODUCTION PROCESSES

Fluid Type	Fluid Properties			Reservoir and Production Processes	Required PVT Tests, Data, and Accuracy				Supplemental Tests		
	Gravity °API	GOR scf/STB	C ₇₊ mol%		Composition	Tests/Equipment/Procedures	Required Data	Data Accuracy			
Heavy Oil	7–25	10–200	> 40	Depletion/ Cold Production	C ₃₀₊ , Wax, and Asphaltene, %	Oil PVT—CCE, DFL, ST	P _o , R _g , B _g , B _o , ρ _o , μ _o F(P, T, Rs)	P _o ±50 psi R _g , μ _o ± 5%; B _o , ρ _o ±2%	Core-depletion tests at different rates Flow tests for relative permeability		
				Solvent Flood		Oil and Oil + Solvent PVT				Same + Changes by solvent addition	
				Waterflood		Oil PVT and Water PVT	Same + B _o , ρ _o , μ _o —F(P)				
				Steamflood		Oil PVT + High-Temperature PVT	Same + Steam properties				
Black Oil	25–35	200–1,500	20–40	Depletion	C ₃₀₊ , Wax, and Asphaltene, %	Oil PVT—CCE, DFL, ST	P _o , R _g , B _g , B _o , ρ _o , μ _o —F(P)	P _o ±50 psi; R _g , μ _o ± 5%; B _o , ρ _o ±2%	Flow tests for relative permeability		
				Waterflood		Oil PVT and Water PVT				Same + B _o , ρ _o , μ _o —F(P)	
				Gasflood— Immiscible		Oil PVT and Oil + Gas PVT	Same + Changes by gas addition				
				HC or CO ₂ Flood—Miscible		Oil PVT and Gas + Oil PVT	Same + P/X data (P _o , μ _o , ρ _o , B _o , Liquid vol%) + Compositional changes with injected gas and P			Same + Liquid vol% ±2%	Relative permeability, slim-tube, and coreflood tests for gas injection
Light Oil	35–40	1,000–2,000	13–20	Depletion	C ₃₀₊ , Wax, and Asphaltene, %	Oil PVT—CCE, DFL, ST	P _o , R _g , B _g , B _o , ρ _o , μ _o —F(P)	P _o ±20 psi; R _g , μ _o ± 5%; B _o , ρ _o ±2%	Flow tests for relative permeability		
				Waterflood		Oil PVT + Water PVT				Same + μ _o , B _o , and B _w —F(P)	
				Gas Injection		Oil PVT + Swelling test	Same + P/X data				
Near-Critical Fluids—Highly Volatile Oil and Rich Condensate	40–50	2,000–5,000	8–13	Depletion	C ₃₀₊ , Wax, and Asphaltene, %	Oil PVT—High Precision	P _o , R _g , B _g , B _o , ρ _o , μ _o —F(P)	Same	Flow tests for relative permeability		
				HC-Gas Injection—Miscible		Oil PVT + Swelling and forward/backward contact test				Same + P/X Data (P _o , μ _o , ρ _o , B _o , and Liquid vol%), and Compositional data with gas injection	Same + Liquid vol% ±2%
				Compositional Gradients		Fluid Compositions With Depth	Same as above + miscibility evaluation of varying oil composition in the reservoir			Same as above	P _o ±20 psi; R _g , μ _o ±5%; B _o , ρ _o ±2%; Liquid vol% ±2%
Gas Condensate	>50	>5,000	< 8	Depletion	C ₂₀₊ , Wax, and Asphaltene, % Water Analysis	Gas-Condensate PVT—CCE, CVD, ST; solubility of gas in water and water vaporization	P _o , Z-factors, CGR, and liquid dropout; PVT changes from water vaporization	P _o ±50 psi; Liquid vol% ±2%; Z-Factor ±2%; CGR ± 1 STB/MMscf	Relative permeability, slim-tube, and coreflood tests for gas injection		
				Gas Injection for Pressure Maintenance		Nonhydrocarbon (N ₂ , CO ₂ , H ₂ S) and Sulfur Analysis				Reservoir-fluid + injection-gas PVT; Special 3-phase PVT-cell with zero dead volume	Same as above + P/X data (P _o , B _g , and CGR changes with injected gas)

reservoir evaluation and development. The PVT-data requirement depends on the fluid type and the expected development and production strategies (Whitson and Brule 2000). **Table 1** provides a list of required PVT data and the needed accuracy for various fluid types and production processes along with general guidelines for designing a laboratory PVT program. For example, extraheavy oils require customized PVT cells and experimental procedures to accelerate the time needed for attaining equilibrium conditions because of the slow gas liberation. On the other hand, more-complex near-critical fluids and miscible-gas-injection processes need special PVT tests and precise measurement techniques to capture the complex phase behavior exhibited by these fluids. Gas condensates in the presence of water require PVT cells that can handle three-phase mixtures of gas, water, and condensate.

Data Quality. Ensuring high-quality data requires routine laboratory visits, evaluation of laboratory procedures and methods, and spot QC as data become available. The QA/QC methods can range from simple graphical techniques to sophisticated material-balance calculations (Whitson and Brule 2000).

Fluid Modeling—Recommended Methodology. Modeling reservoir-fluid PVT behavior is necessary for reservoir-engineering calculations and simulation studies. Several approaches including black-oil correlations, pseudocompositional formulations, and fully compositional equation-of-state (EOS) methods are used to develop fluid models. Most black-oil correlations are based on regional fluid data, and, therefore, caution should be exercised in choosing cor-

relations for specific oils. Also, it should be recognized that as these correlations are based on measured data and lack a thermodynamic basis, extrapolation outside the range of data might contribute to large errors. However, EOS models based on thermodynamic principles are useful for reasonable extrapolation beyond the data range (Whitson and Brule 2000). When cost and computational considerations dictate use of black-oil models for simulation studies, it is highly recommended to derive black-oil properties by use of EOS fluid models tuned to laboratory data (Whitson and Brule 2000). EOS-based fluid modeling involves several critical steps including optimum-component selection by means of C₇₊ characterization, incorporation of robust phase-equilibrium calculation (energy minimization) and solution techniques to ensure convergence, and a rigorous regression method to tune the model to laboratory data. A brief discussion of these techniques is provided, and their applications are demonstrated through examples.

C₇₊ Characterization and Component Selection. The C₇₊ fraction of the reservoir fluid contains numerous compounds of different homologues (paraffinic, naphthenic, and aromatic) and plays a dominant role in determining the PVT behavior of the fluid. For example, in a gas-condensate fluid, the dewpoint pressure is a strong function of C₇₊ molecular weight and its relative amount in the fluid. In heavy oils, C₇₊ components dictate the viscosity behavior and control the asphaltenes- and wax-deposition characteristics. Similarly, in volatile oils and rich condensates, the oil volumes and other properties below the saturation pressure are determined by the amounts of intermediate and heavy components.

TABLE 2—FIELD EXAMPLES OF FLUID SAMPLING AND CHARACTERIZATION

Fluid type/ Process	Reservoir	Pressure, psia	T, °F	Gravity, °API	GOR, scf/STB	Issues	Methods
Extraheavy oil	Cerro Negro	1,400	130	8–9	120–130	Sampling, PVT measurements	Formation-fluid sampling, special apparatus and procedures
Black oil/CO ₂ flooding	Salt Creek	2,500	124	34	415	Extended PVT tests, detailed fluid characterization	Customized tests, models by rigorous techniques
Near-critical-fluid/ Miscible-HC-gas injection	Oso	6,300	232	40–45	2,500 to 4,000	Sampling, high-precision measurements, modeling compositional gradients	Formation-fluid sampling, special apparatus, gradient modeling
Gas Condensate	Arun	7,100	352	55	20,000	Water and reservoir-fluid PVT, corrosion	Special PVT tests, customized modeling

Therefore, it is important to characterize them accurately. Several techniques are used to lump these components into pseudocomponents for EOS models. The most widely used method is from Whitson (1983) in which the C_{7+} distribution is represented by a continuous gamma distribution that is optimally discretized into a few fractions (i.e., pseudocomponents). Fluid type and the production processes involved further dictated the component selection. When describing near-critical fluids and miscible processes, it is important to have more intermediate and volatile components in the fluid description to mimic simple revaporization and more-complex condensing and vaporizing drives. Specifics of component selection will be highlighted through examples.

Energy Minimization and Model Optimization. Although EOS-based fluid models predict multicomponent phase behavior reliably, they still lack the capability to mimic near-critical behavior because of mathematical singularities encountered in this region. Therefore, more-rigorous methods such as Gibbs/Helmholtz energy minimization and robust solution techniques are needed to model near-critical behavior (Nagarajan et al. 1991). Application of these techniques is discussed under various examples. Another critical step in fluid modeling is optimizing model parameters to match measured data. Generally, an EOS fluid model uses 6 to 12 components, of which four to five are C_{7+} pseudocomponents. The result is several tens of model parameters (such as component-critical properties—critical pressures, temperatures, volumes, and acentric factor—and several binary interaction coefficients) to be regressed on. Systematic grouping of these parameters is essential for reliable and faster regression.

Field Examples

The fluid-characterization steps discussed above are illustrated through field examples ranging from heavy oils to lean gas condensates as listed in **Table 2** along with relevant fluid parameters, fluid-characterization challenges, and solutions.

Heavy Oil—Cerro Negro Field. The Cerro Negro field in the Orinoco oil belt in northeastern Venezuela contains

extraheavy oil in highly unconsolidated sands. The average reservoir pressure and temperature range between 800 and 1,450 psia and 120 and 145°F, respectively. The stock-tank oil gravity is approximately 9°API. The live-oil viscosity ranges from 600 to 3,000 cp at reservoir conditions. The solution GOR of the oil is 120 to 130 scf/STB. The high oil viscosity impedes the separation of solution gas from the oil below its true bubblepoint pressure, resulting in microbubbles of gas dispersed in the oil until diffusion forces help the gas bubbles to coalesce slowly into a distinct gas phase (Cengiz et al. 2004). This unique behavior poses several challenges in fluid sampling and PVT measurement requiring careful choice of tools and procedures.

Sampling Method, Tools, and Procedures. The objective of the heavy-oil sampling program was to obtain adequate volumes of representative single-phase oil samples for laboratory analysis. The following sampling challenges had to be addressed (Reddie and Robertson 2004): adequate near-wellbore cleaning to minimize sample contamination by drilling-mud filtrate and optimal drawdown to minimize sand production and avoid two-phase flow while mobilizing the oil from the reservoir into the sample chamber. During surface sampling, measurement uncertainty in the producing GOR is a concern because of large drawdown and incomplete gas separation from the oil. Another challenge with surface samples is the slow dissolution of gas while recombining them to prepare reservoir fluid. Many of these sampling problems can be eliminated by use of bottomhole sampling with a wireline formation tester having appropriate tool selection and procedures as identified in **Table 3**.

The key components of a wireline-formation-tester tool include a variable-rate pump-out module, properly sized screens to prevent plugging of flow lines by sands and fines, a resistivity cell, and two optical fluid analyzers to monitor fluid quality and detect two-phase conditions. Single-phase sample bottles should be used for sample collection to avoid flashing the samples. The main advantage of bottomhole sampling over surface sampling is that the former offers a viable means to capture single-phase samples and eliminate uncertainties associated with surface samples.

TABLE 3—WFT TOOL DESIGN FOR HEAVY-OIL SAMPLING			
Problem/Issue	Requirement	Tool Selection	Design/Configuration
Sand production and two-phase flow when mobilizing oil	Optimal drawdown, Control sand production	Dual-packer option, Flow-control pump, Coarse/fine filters	Pump configured close to sampling point
Mud-filtrate contamination	Adequate pumpout volume before sampling	Pump with variable rate (high to low)	High rate: cleaning, Low rate: sampling
Fluid quality	Fluid-quality monitoring, Identify contaminants	Optical fluid analyzers, Resistivity cell	Fluid analyzers positioned above and below pump
Single-phase samples adequate volumes	Sample-bottle type, volume, and number	Single-phase sample bottles	Close to sampling-point location

A sampling-simulation program was used to estimate optimum pumping rates to minimize the probability of sand production while mobilizing the oil under single-phase conditions. By use of estimated reservoir and fluid parameters, the pump-out volume and time required for adequate cleaning also were estimated. Specific sampling procedures were developed to reduce the possibility of collecting nonrepresentative samples. In addition, procedures for on-site sample transfer and shipping were developed to preserve sample integrity. Qualified personnel were on site to coordinate and monitor the entire sampling operation. As a result, several high-quality samples were captured for detailed compositional and PVT analysis.

PVT Measurements and Modeling. Because of slow gas liberation and dissolution in this heavy oil, special care was exercised in selecting equipment and procedures for sample preparation and PVT measurements (Cengiz et al. 2004). The sample preparation involved removing both free and emulsified water from the samples by a nonchemical method. The dewatering process consisted of pressurizing the sample above the reservoir pressure and subjecting it to repeated heating and cooling cycles from room temperature

to double the reservoir temperature, resulting in water content of less than 1% in the oil.

A direct-mixing PVT cell was custom designed to facilitate faster equilibrium during PVT measurements, especially for measuring the bubblepoint. However, even with this PVT cell, nonequilibrium measurements were likely if proper experimental procedures were not followed. In an equilibrium test, the pressure/volume curve exhibits a sharp change in the slope at the bubblepoint. However, as Fig. 2a shows, it is difficult to detect such sharp slope changes in a nonequilibrium test (Cengiz et al. 2004). Monitoring pressure response as a function of time and its rate of change in both nonequilibrium (without stirring) and equilibrium (with vigorous stirring) tests, as shown in Fig. 2b, would help identify true equilibrium conditions. A sharp drop in pressure (Segment 1 in Fig. 2b) was observed as soon as the cell volume was expanded, indicating the behavior of an incompressible liquid. As the gas slowly evolved, a gradual pressure buildup (Segment 2) was observed, but equilibrium condition was not reached even after 20 hours without stirring. However, with vigorous mixing, equilibrium condition was reached rapidly as indicated by Segments 3 and 4 in Fig. 2b. By this

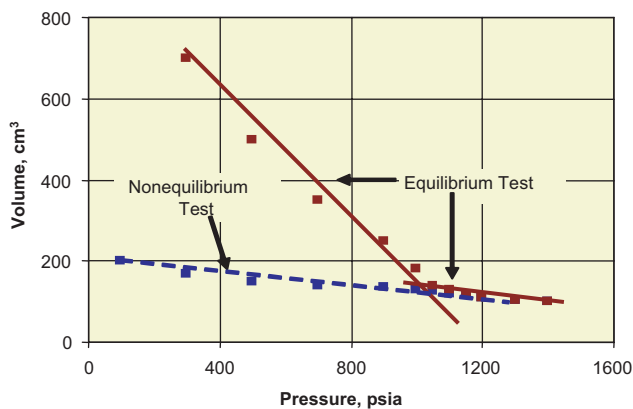


Fig. 2a—Equilibrium and nonequilibrium heavy-oil bubblepoint measurement.

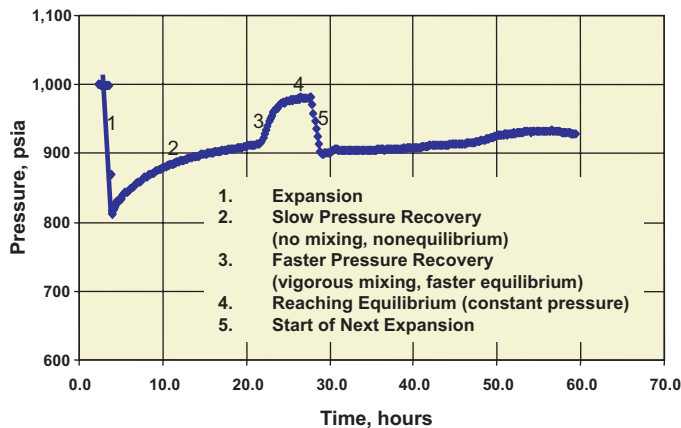


Fig. 2b—Pressure response vs. time near bubblepoint equilibrium and nonequilibrium behavior.

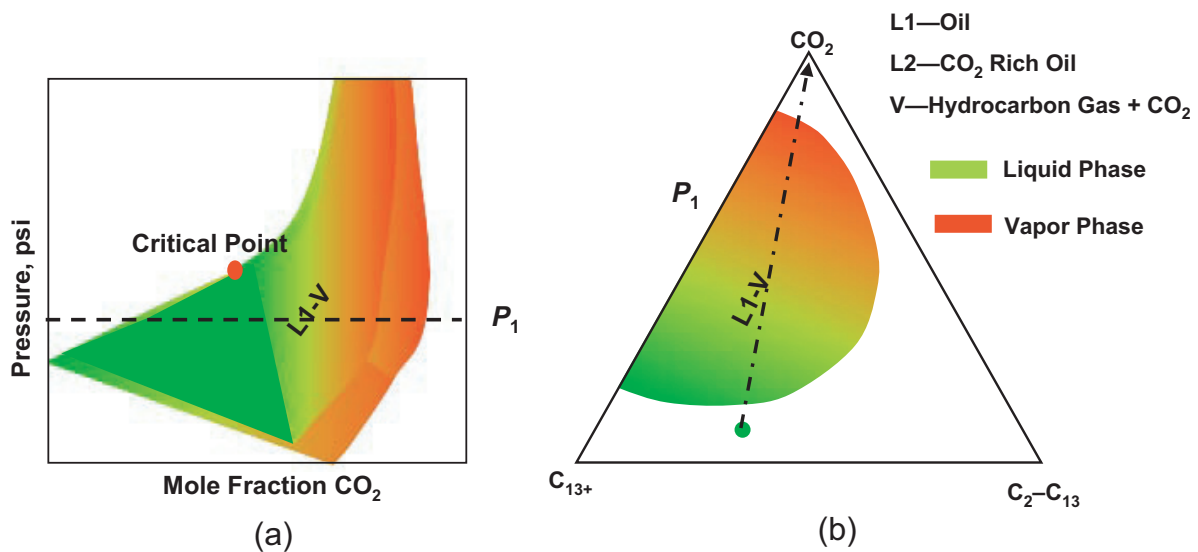


Fig. 3—CO₂+oil pressure/composition and ternary diagrams at T>120°F.

approach of ensuring equilibrium, the true bubblepoint pressure was measured repeatedly within approximately 50 psi. Similar procedures were followed in other PVT tests.

A capillary-flow viscometer was used to measure the oil viscosity. Because the oil is saturated at each pressure step in the differential-liberation experiment, small pressure drops in the capillary viscometer caused by the flow will liberate the gas. Therefore, it was necessary to conduct several viscosity measurements above the saturated pressure and use an extrapolation technique to determine the viscosity at the desired differential-liberation pressure.

PVT-data interpretation and modeling for heavy oils require reliable pseudoization of C₇₊ components because a majority of components in heavy oils fall in this range (Romero et al. 2001). Solid-forming compounds, such as wax and asphaltenes, should be characterized properly for flow assurance needs. Rigorous viscosity models that corre-

late viscosity as functions of pressure, temperature, and GOR are needed to capture large variations of heavy-oil viscosity throughout the operating conditions.

Black Oil—Salt Creek Reservoir. The Salt Creek field in west Texas is a carbonate reservoir in the Permian Basin containing medium-gravity oil (35°API). The initial reservoir pressure and temperature were 2,199 psia and 124°F, respectively. The initial GOR of the oil was 415 scf/STB and the live-oil viscosity was 0.8 cp. The fluid exhibited a bubblepoint pressure of 1,620 psia at 124°F. The reservoir was initially produced by depletion, pressure maintenance, and gas recycling, followed by waterflood and infill drilling (Bishop et al. 2004). High remaining oil saturations in several parts of the reservoir after waterflood prompted an evaluation of CO₂-miscible-flooding potential to recover some of the remaining oil. Significant solubility of CO₂ in the

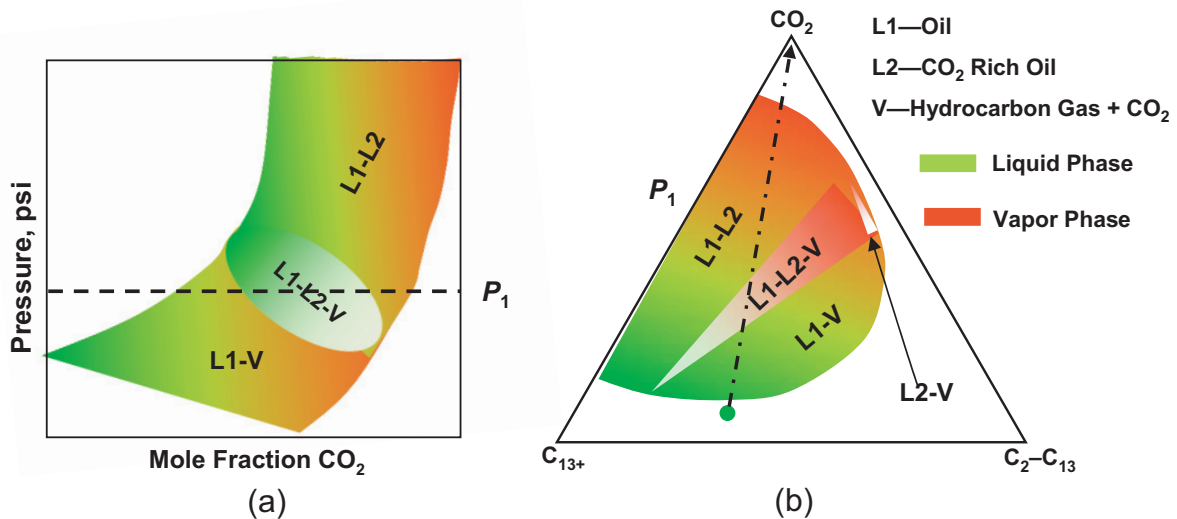


Fig. 4—CO₂+oil pressure/composition and ternary diagrams at T<120°F.

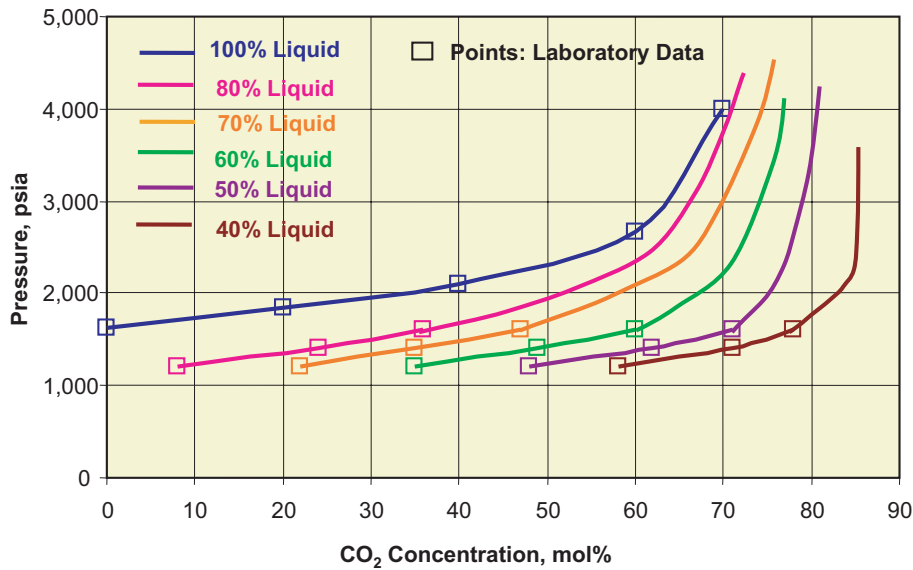


Fig. 5—Swelling-test data for CO₂ miscible process.

oil enhances the recovery through oil swelling and viscosity reduction (Stalkup, 1984). CO₂ also vaporizes intermediate components leading to multicontact miscibility and high recoveries (Stalkup, 1984). A systematic PVT-data-acquisition and modeling study was undertaken for Salt Creek to evaluate recovery efficiency to CO₂ flooding.

CO₂+Oil Phase Behavior. A typical phase behavior exhibited by CO₂+oil mixtures at both high (>120°F) and low (<120°F) temperatures, respectively, is displayed in **Figs. 3 and 4** through pressure/composition (P/X) and ternary diagrams (Bishop et al. 2004). Depending on the pressure, temperature, and composition, CO₂+oil mixtures can exhibit near-critical behavior including multiphase equilibrium ranging from simple two-phase liquid/vapor (Figs. 3a and 3b) to more-complex two- or three-phase liquid/liquid or liquid/liquid/vapor equilibrium (Figs. 4a and 4b). As shown in Fig. 3, the CO₂+oil phase boundary in the critical region is steep. The fluid properties also vary significantly in this region with small changes in operating conditions or fluid composition. PVT tests for evaluating CO₂-injection processes should be designed to acquire high-precision compositional and PVT data for modeling this complex phase behavior. The data interpretation and modeling are equally challenging.

PVT Data Requirement. The basic PVT tests comprised constant-composition expansion, differential liberation, and multistage-separator tests to describe the oil PVT behavior as a function of reservoir and surface conditions. Additional PVT tests including swelling-test and multicontact experiments, and slim-tube and coreflood tests were conducted to acquire both equilibrium PVT data on CO₂+Salt Creek oil mixtures and dynamic-flow data with CO₂ as displacing fluid. Several CO₂+oil mixtures with CO₂ concentrations ranging from a few mole percent to as high as 70 mol% were used in swelling tests measuring saturation pressures, density, and viscosity as functions of pressure and CO₂ concentration. The liquid/vapor volume fractions and composi-

tions in the two-phase region also were measured at several pressures as functions of CO₂ concentration. **Fig. 5** shows a measured P/X diagram for liquid-volume changes as a function of both pressure and composition. In slim-tube tests, the effluent-fluid compositions were measured in addition to the conventional measurement of recovery and gas breakthrough. This information was used for dynamic tuning of the reservoir-fluid model for simulation. The minimum miscibility pressure for CO₂ injection, the residual-oil saturation for miscible flood, and the effluent-fluid compositions were measured in a series of flow tests.

Fluid Modeling. To model Salt Creek CO₂ processes, it was necessary to split the C₇₊ fraction into a large number of pseudocomponents for the EOS model. Pseudocomponents were generated by lumping components in small ranges of carbon numbers (e.g., C₇–C₉, C₁₀–C₁₃, C₁₄–C₁₆, ...). This type of detailed C₇₊ description was necessary to capture vaporization of intermediate components as high as C₂₀ to C₂₅ by the dense CO₂-rich phase. A Helmholtz energy-minimization procedure in terms of molar densities was used to identify correct phase equilibrium solutions (Nagarajan et al. 1991). The Helmholtz energy minimization formulation converges to true solutions by avoiding difficulties encountered while using Gibbs energy-minimization as functions of mole numbers and molar volume. Predicted P/X diagram and liquid volumes agreed well with the measurements, as shown in Fig. 5. In addition to tuning the fluid model to equilibrium PVT data, the slim-tube and coreflood data were used in a 1D simulator to fine-tune the EOS model under flow conditions.

Near-Critical Fluid—Oso Field. The 2Y2 reservoir of the Oso field offshore Nigeria contains a highly undersaturated near-critical fluid (El-Mandouh et al. 1993). The initial reservoir pressure and temperature were 6,300 psia and 232°F, respectively. The high relief of the reservoir and the near-

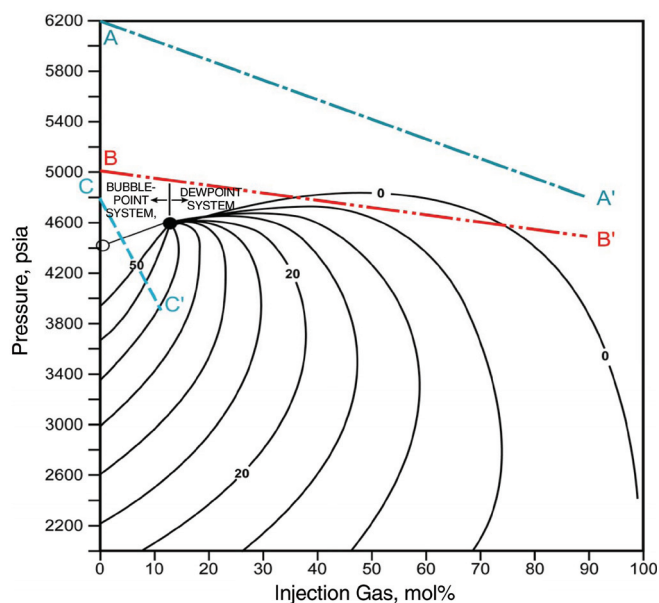


Fig. 6—Oso fluid and injection-gas phase diagram.

critical nature of the fluid contributed to substantial fluid gradients with depth. Early in the development planning, hydrocarbon-gas injection was identified as a necessary production scheme for pressure maintenance and improved recovery through near-miscible processes.

Several key fluid-characterization issues were investigated for their effect on recovery factors as part of scoping, planning, and development studies. Fluid characterization addressed the following issues:

- Acquisition of representative samples at various depths to quantify initial fluid gradients and for PVT studies.
- PVT measurements to capture near-critical behavior, evaluate gas-injection strategies, and design the surface-separator train.
- Fluid modeling to predict observed near-critical behavior and property changes during gas injection.
- Development of thermodynamically consistent compositional-gradient models for use in reservoir studies.

Sampling. Sampling Oso reservoir fluid posed significant challenges because the fluid was near-critical. The near-critical nature of the fluid required careful design and execution of sampling because small variations in the fluid pressure and temperature can cause significant changes in fluid composition, particularly near the saturation pressure. Representative fluid sampling required strict isolation of sampling intervals because the fluid properties varied over depth. During the surface-sampling operation, low drawdown, complete phase separation in the surface equipment, and accurate measurement of oil and gas rates were critical for obtaining representative GOR for laboratory recombination. Both bottomhole wireline-formation-tester- and surface-sampling methods were used to collect several reservoir-fluid samples from different depths.

PVT Data Requirement. Near-critical PVT measurements required expertise in measuring, analyzing, and interpreting the data in addition to state-of-the-art PVT equipment.

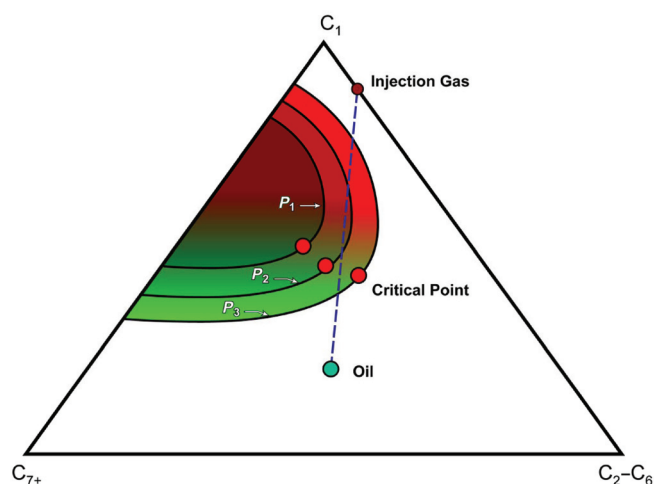


Fig. 7—Ternary diagram for Oso fluid and injection gas.

Longer equilibration times and high-precision measurements were necessary to capture steep changes in fluid properties that occurred with small changes in pressure, temperature, or composition. A swelling test was conducted to define the P/X phase-boundary and fluid-property changes resulting from gas injection. The measured-P/X diagram of Oso fluid with injection gas in Fig. 6 shows that with small additions of injected gas, the in-situ fluid is in a critical region. Ternary diagrams at several intermediate pressures ($P_1 > P_2 > P_3$) constructed with measured swelling data and EOS calculations are shown in Fig. 7. These diagrams were used to evaluate various injection strategies.

The reservoir pressure at which gas injection begins, along with the injection and production rates, affect the thermodynamic path taken by the reservoir fluid during depletion and, hence, the resulting recovery mechanism. For example, if gas injection begins at the initial reservoir pressure of 6,300 psia and production takes the path marked A–A' in Fig. 6 and the corresponding two-phase region marked P_1 in Fig. 7, the hydrocarbon fluid will remain a single-phase throughout the injection process, leading to a first-contact miscible process. During this process, the fluid changes from a volatile oil to a gas condensate as it crosses the critical region in a single-phase state. However, if the injection begins at a lower pressure, P_2 , the fluid enters the two-phase region to the right of the critical point close to the cricondenbar, path B–B' in Fig. 6 and the ternary diagram corresponding to P_2 in Fig. 7. As the fluid enters the two-phase region, a small amount of oil will drop out. As gas injection continues, this oil will re-evaporate and will be recovered at the surface. Finally, if the gas injection begins at a lower pressure, P_3 the fluid enters the two-phase region along path C–C' in Fig. 6 to the left of the critical point and the corresponding ternary diagram at P_3 in Fig. 7. In this process, multicontact miscibility will develop. As gas injection continues, the faster-moving gas phase will be continually enriched by vaporizing intermediate components (vaporizing-gas drive) until the gas phase becomes first-contact miscible with the oil. This analysis was used to optimize the development plan.

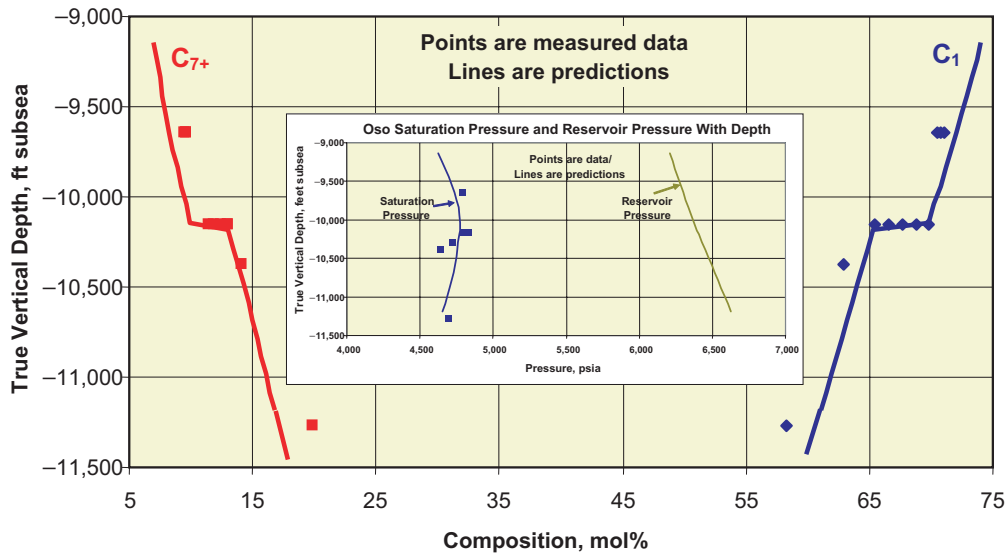


Fig. 8—Compositional-gradient and fluid-property variations as a function of depth—Oso.

Fluid Modeling. The near-critical nature of Oso fluids, coupled with strong compositional gradients, demands robust compositional fluid models (Høier and Whitson 2001). An EOS fluid model was developed following similar steps outlined in the previous example. The C_{7+} fraction was divided into an adequate number of volatile components to capture the near-critical behavior. The EOS calculations were performed with energy minimization and robust solution techniques (Nagarajan et al. 1991). The EOS model also was required to capture observed compositional gradients, which was accomplished by modifying the chemical-equilibrium equation to include the gravitational effect through a gravity/chemical equilibrium model (Høier and Whitson 2001). The compositional gradients and the resulting fluid-property variations were predicted by use of the gravity/chemical

equilibrium model in the EOS and the results are shown in **Fig. 8**. The predicted methane and C_{7+} compositional variations agreed well with the data. The inset in **Fig. 8** shows that computed saturation-pressure variations with depth agree with laboratory measurements. The PVT data and the EOS model were used to provide guidelines for designing surface-separator trains. Because of the near-critical nature of the fluid, the number of separator stages and the stage-separator pressures had to be optimized to maximize recovery of surface liquids. A series of multistage-separator simulations were performed to evaluate sensitivity of the liquid yield to the number of stages and stage pressures. **Fig. 9** shows the sensitivity of liquid yield to the number of stages and the stage pressures. Two to four stages of separation are necessary to maximize recovery of surface liquids. However, increasing

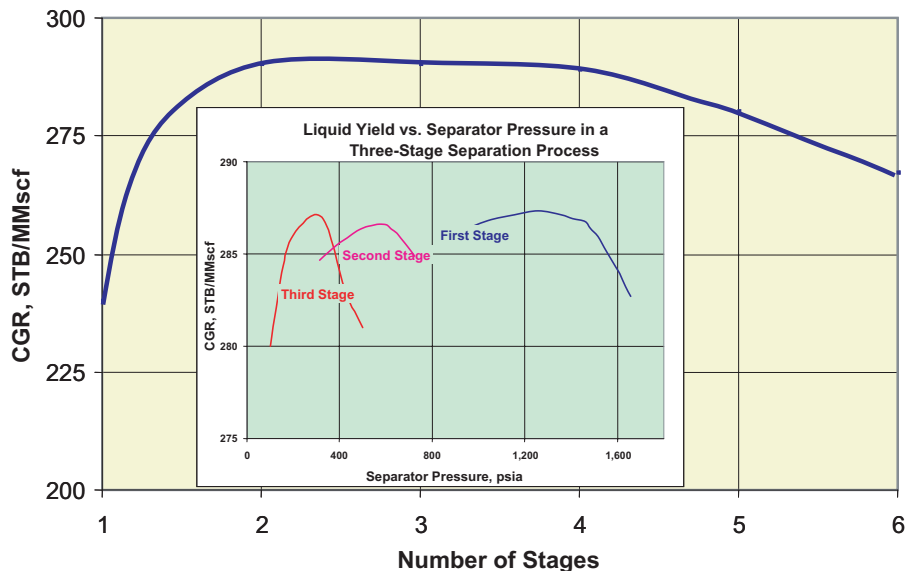


Fig. 9—PVT-based separator design to maximize liquid yield—near-critical-fluid example.

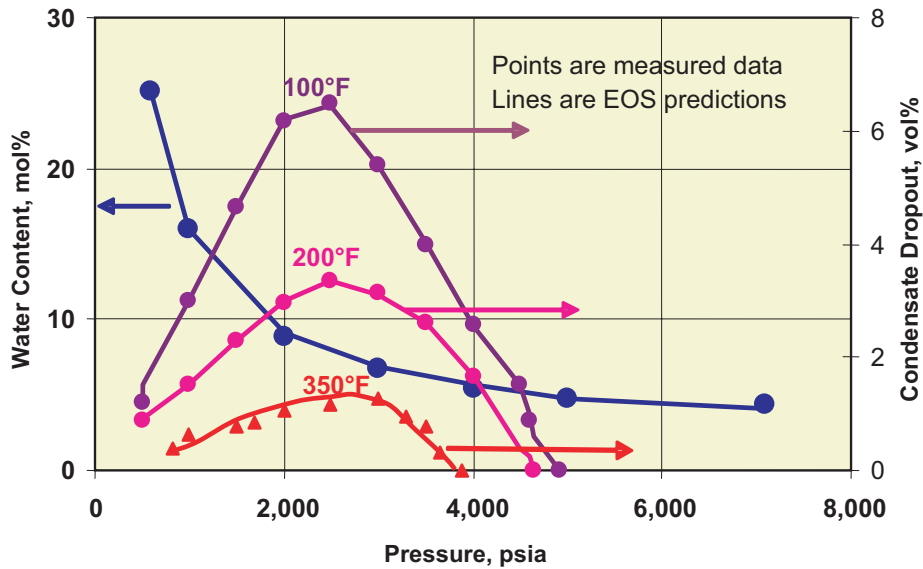


Fig. 10—Water content and condensate-dropout characteristics of Arun gas.

the number of stages beyond four affected the yield negatively. In addition, Fig. 9 shows that if a three-stage-separator train is selected, the second- and third-stage pressures must be selected precisely to maximize surface-liquid recovery.

Gas Condensate—Arun Field. The Arun Field in Indonesia is a high-temperature lean-gas-condensate reservoir with surface-liquid yields of approximately 50 to 55 STB/MMscf (Pathak et al. 2004). The original reservoir pressure was 7,100 psig at 352°F. Initially, Arun gas contained significant amounts of vaporized water (4 mol%) and CO₂ (16 mol%). Accurate characterization of gas-condensate/water phase behavior through an EOS was essential to predict water-production levels and corrosion potential.

PVT Data and Model. A PVT program was initiated to study gas/water and gas-condensate/water phase behavior as functions of pressure and temperature (Ng and Robinson 1986; Ng et al. 1988). A specially designed visual PVT cell was used to measure the amount of water vapor in the gas phase and the condensate/water volumetric behavior as a function of reservoir, wellbore, and surface conditions. The results showed that water content of the reservoir gas increased four-fold from approximately 4 mol% at 7,100 psig to approximately 16 mol% at 1,000 psig as shown in Fig. 10 (Ng and Robinson 1986). This relation corresponds to water production increasing from 6.5 STB/MMscf at the initial reservoir conditions to 75 STB/MMscf as the reservoir pressure declined to 1,000 psig (Pathak et al. 2004). This information is critical for designing optimum water-handling facilities and for corrosion management. Fig. 10 also shows condensate dropout at different reservoir, wellbore, and surface conditions, indicating an initially increasing condensate dropout with declining pressure and temperature, peaking approximately 2,500 psia, and dropping off at lower pressures as a result of condensate revaporization (Ng et al. 1988).

Fig. 11 combines the volumetric behavior of condensate and water in terms of condensate/water ratio (CWR) at the

bottomhole (352°F), wellhead (200°F), and surface (100°F) temperatures during reservoir depletion. Generally, the CWR is controlled by the condensate-dropout characteristics during the early stages of depletion. But, as the reservoir pressure declines below dewpoint pressure, the CWR falls more rapidly as a result of decreasing condensate volume (caused by liquid dropout in the reservoir) and increasing water volume (caused by increased water vaporization). In Fig. 11 at 352°F, the condensate volume is zero until the reservoir pressure drops below the dewpoint pressure, then it increases with declining reservoir pressure, going through a maximum, and finally decreasing as a result of revaporization at lower pressures. The water volume, however, increases slowly at first and then rapidly as a result of an increased rate of water vaporization at lower pressures and subsequent condensation in the wellbore. At 200°F (wellhead) in Fig. 11, the condensate volume initially increases as a result of both the pressure and temperature drop in the wellbore. However, increased water vaporization during reservoir depletion and subsequent condensation at the wellhead cause a larger increase in water volume resulting in a sharp drop in CWR. At 100°F (surface), the CWR behaves in a similar manner as at the wellhead. However, the crossover of condensate and water volumes (CWR =1) occurs at the surface (pink curve) much earlier (reservoir pressure of 4,000 psia) than at the wellhead, green curve (reservoir pressure 2,800 psia). The implication is that the potential for corrosion is high in the surface equipment in the early stages of depletion. The corrosion potential may increase toward the wellhead and downhole with reservoir pressure decline.

In the Arun reservoir, water vaporization and three-phase water/condensate/gas volumetric behavior were modeled with a three-parameter Peng-Robinson EOS. Because a cubic equation does not model a polar compound such as water accurately, the critical properties of water were modified on the basis of the coordination number to match laboratory data. Further, special binary-interaction parameters for water

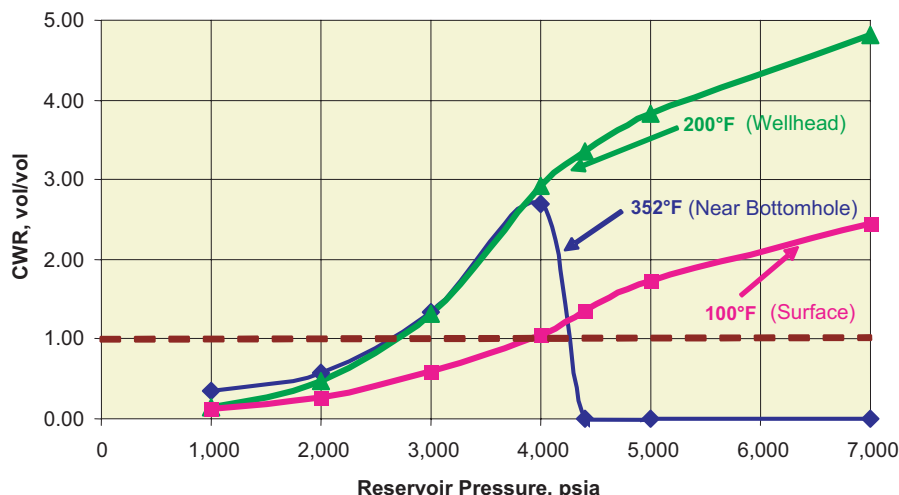


Fig. 11—CWR of produced gas in the wellbore as reservoir pressure declines.

were used in the tuning process. The EOS-model matches are shown in Figs. 10 and 11 as solid lines.

Conclusions

Fluid characterization strongly affects in-place-volume, recovery-factor, injectivity/productivity, and well-deliverability calculations. Accurate fluid characterization minimizes technical uncertainties and, thus, provides a reliable representation of the asset value. Four field examples containing fluids from extraheavy oil to lean gas condensates undergoing different production processes were presented to highlight key steps in fluid sampling and characterization.

1. Fluid-sampling programs must be tailored to the fluid type, reservoir-rock and -fluid conditions, and fluid distribution. Special tools and procedures with strict QC will ensure obtaining high-quality representative samples.
2. The fluid type and production processes dictate PVT-data requirements, measurement methods, and data accuracy. Laboratory methods and procedures must be tailored to specific fluids with expert QA/QC.
3. The C₇₊ components must be characterized accurately for EOS-component selection. Rigorous modeling methods, such as energy minimization, and robust solution techniques are needed to model near-critical fluids and processes.
4. Reliable compositional-gradient models are needed to capture fluid-property variations in reservoirs with high relief and/or near-critical fluids.

Acknowledgments

We gratefully acknowledge the support and encouragement of ExxonMobil Upstream Research Company, ExxonMobil Production Company, ExxonMobil Oil Indonesia, Mobil Producing Nigeria, and ExxonMobil de Venezuela.

Acronyms

- CCE = constant-composition expansion
- CGR = condensate/gas ratio
- CVD = constant-volume depletion
- CWR = condensate/water ratio

- DFL = differential liberation
- DST = drillstem test
- EOS = equation of state
- GOR = gas/oil ratio
- HC = hydrocarbon
- OBM = oil-based mud
- PVT = pressure/volume/temperature
- P/X = pressure/composition
- QA = quality assurance
- QC = quality control
- ST = separator test

Nomenclature

- B_o = oil formation volume factor
- B_g = gas formation volume factor
- B_w = water formation volume factor
- F(P) = function of pressure
- F(T) = function of temperature
- F(R_s) = function of solution gas/oil ratio
- p = pressure
- p_b = bubblepoint pressure
- p_d = dewpoint pressure
- R_s = solution GOR
- T = temperature
- V_l = volume of liquid
- Z = gas deviation factor
- μ_o = viscosity of oil
- μ_w = viscosity of water
- ρ_o = density of oil
- ρ_w = density of water

References

Bishop, D.L., Williams, M.E., Gardner, S.E., Smith, D.P., and Cochrane, T.D. 2004. Vertical Conformance in a Mature Carbonate CO₂ Flood: Salt Creek Field Unit, Texas. Paper SPE 88720-MS presented at the SPE Abu Dhabi International Petroleum Exhibition and Conference, Abu Dhabi, UAE, 10–13 October. DOI: 10.2118/88720-MS.

-
- Cengiz, S., Robertson, C., Kalpacki, B., and Gupta, D. 2004. A Study of Heavy Oil Solution Gas Drive for Hamaca Field: Depletion Studies and Interpretations. Paper SPE 86967-MS presented at the SPE International Thermal Operations and Heavy Oil Symposium and Western Regional Meeting, Bakersfield, California, 16–18 March. DOI: 10.2118/86967-MS.
- El-Mandouh, M.S., Bette, S., Heinemann, R.F., Ogamien, E.B., and Bhatia, S.K. 1993. Full-Field Compositional Simulation of Reservoirs of Complex Phase Behavior. Paper SPE 25249-MS presented at the 12th SPE Symposium on Reservoir Simulation, New Orleans, 28 February–3 March. DOI: 10.2118/25249-MS.
- Hoier, L., and Whitson, C.H. 2001. Compositional Grading—Theory and Practice. *SPE* **4**(6): 525. SPE 74714-PA. DOI: 10.2118/74714-PA.
- Honarpour, M.M., Nagarajan, N.R., and Sampath, K. 2006. Rock/Fluid Characterization and Their Integration—Implication on Reservoir Management. *JPT* **58**(9): 120. SPE 103358-MS. DOI: 10.2118/103358-MS
- Nagarajan, N.R., Cullick, A.S. and Griewank, A. 1991. New Strategy for Phase Equilibrium and Critical Point Calculations by Thermodynamic Energy Analysis; Part I. Stability Analysis and Flash; Part II. Critical Point Calculations. *Fluid Phase Equilibria* **62**(3): 211.
- Ng, H.-J., and Robinson, D.B. 1986. The Influence of Water and Carbon Dioxide on the Phase Behavior and Properties of a Condensate Fluid. Paper SPE 15401 presented at the SPE Annual Technical Conference and Exhibition, New Orleans, 5–8 October. DOI: 10.2118/15401-MS.
- Ng, H.-J., Robinson, D.B., Nagarajan, N.R., Rastogi, S.C., and Hasan, N. 1988. Phase Behavior of Retrograde Gas Condensate-Water System Under High Pressure and Temperature Conditions. Paper presented at the Indonesian Petroleum Congress, Jakarta.
- Pathak, P., Fidra, Y., Kahar, Z., Agnew, M., and Hidayat, D. 2004. The Arun Gas Field in Indonesia: Resource Management of a Mature Field. Paper SPE 87042-MS presented at the SPE Asia Pacific Conference on Integrated Modelling for Asset Management, Kuala Lumpur, 29–30 March. DOI: 10.2118/87042-MS.
- Reddie, D.R. and Robertson, C.R. 2004. Innovative Reservoir Fluid Sampling Systems. Paper SPE 86951-MS presented at the SPE International Thermal Operations and Heavy Oil Symposium and Western Regional Meeting, Bakersfield, California, 16–18, March. DOI: 10.2118/86951-MS.
- Romero, D.J., Fernandez, B., and Rojas, G. 2001. Thermodynamic Characterization of a PVT of Foamy Oil. Paper SPE 69724-MS presented at the SPE International Thermal Operations and Heavy Oil Symposium, Parlar, Margarita Island, Venezuela, 12–14 March. DOI: 10.2118/69724-MS.
- Stalkup Jr., F.I. 1984. *Miscible Displacement*. Henry Doherty Monograph Series. SPE of AIME: Richardson, Texas. **8**.
- Whitson, C.H. 1983. Characterizing Hydrocarbon Plus Fractions. *SPEJ* **23**(4): 683. DOI: 10.2118/12233-PA
- Whitson, C.H. and Brule, M. 2000. *Phase Behavior*: Monograph Series. SPE: Richardson, Texas. **20**.
- Witt, C.J. and Crombie, A. 1999. A Comparison of Wireline and Drillstem Test Fluid Samples From a Deep Water Gas-Condensate Exploration Well. Paper SPE 56714-MS presented at the SPE Annual Technical Conference and Exhibition, Houston, 3–6 October. DOI: 10.2118/56714-MS. **JPT**